

A dual band Y-shape monopole antenna for 5G wireless application

MD. ZIKRUL BARI CHOWDHURY¹, AMMAR ARMUGHAN², MOHAMMAD TARIQUL ISLAM^{1,*}, ISMAIL HOSSAIN³, MD. NAIMUR RAHMAN^{4,*}, MD. MONIRUZZAMAN⁵, SARNA MAJUMDER⁴, MD SAMSUZZAMAN^{4,6,*}

¹Dept. of Electrical, Electronic and Systems Engineering, Faculty of Engineering and Built Environment, Universiti Kebangsaan Malaysia, Malaysia

²Department of Electrical Engineering, College of Engineering, Jouf University, Sakaka 72388, Saudi Arabia

³Space Science Center (ANGKASA), Universiti Kebangsaan Malaysia, 43600 UKM Bangi, Selangor, Malaysia

⁴Faculty of Computer Science and Engineering, Patuakhali Science and Technology University, Bangladesh

⁵Dept. of Electrical and Electronics Engineering, International University of Business, Agriculture and Technology (IUBAT), Bangladesh

⁶Department of General Educational Development (GED), Faculty of Science and Information Technology (FSIT), Daffodil International University, Dhaka, Bangladesh

In this paper, a novel dual-band Y-shaped monopole patch antenna is proposed, designed, and fabricated for a 5G wireless application. The radiator patch of the antenna's wide and length was fabricated on an FR-4 substrate with the dimension of the proposed antenna of 27.88×23.67×1.58 mm³. The CST studio suite is utilized for all the virtual simulations and analyses regarding fabricated antennas. The study reveals that the fabricated antenna has a bandwidth of 6.20 GHz, covering 3.20-4.60 GHz and 5.10-9.90 GHz frequency ranges, respectively. The antenna has a nice S₁₁ characteristic, excellent impedance matching, and an almost omnidirectional radiation pattern. The S₁₁ is observed at -23.30 dB, and -26.60 dB for the resonant frequency of 3.75 GHz and 7.10 GHz, correspondingly, which covers two Malaysian 5G, frequency bands. The peak gain is 4.78 dB, and the maximum efficiency is 92%, accordingly to the whole frequency band. The VSWR is ideal at 1.02. Finally, the proposed antenna is an attractive solution for 5G wireless communication.

(Received August 11, 2022; accepted June 9, 2023)

Keywords: 5G, wireless communications, Patch antenna, FR-1, N77, Gain, Efficiency, Radiation patterns

1. Introduction

5G is one of the most advanced technologies in the world today. Everyone is curious about this technology. It offers several advantages, including seamless coverage, high data rates, low latency, and excellent reliability [1, 2]. The requirement for higher bandwidth speeds has increased, and within the next few years, it is expected that migration from the current generation to a higher generation, and hence to a higher frequency band, will be needed [3]. Microstrip patch antennas are an appropriate solution for 5G applications that operate at higher frequency ranges. Moreover, microstrip patch antennas are low-cost, lightweight, and cheap to fabricate. The size of the device reduces as the frequency increases. As a result, the antennas are usually miniaturized and compact so that they may be used in various smart devices. The frequency spectrum is an essential part of every communication. These are divided into three categories as a low-frequency band, medium-frequency band, and high-frequency band. 5G communication technology operates at low, mid, and high frequencies to obtain increased bandwidth and system capacity in dense deployments, depending on the use and applications [4]. In Malaysia, for 5G technology, five

pioneer bands have been assigned. These are 3.5 GHz, 5.9-7.1 GHz, 27.5-28.35 GHz, 37-37.6 GHz and 64-71 GHz. The proposed antenna covers n77 (3.3–4.2) GHz and FR1 (4.4–7.1) GHz 5G frequency bands. The lower frequencies have been widely analyzed, and it is expected that they provide better coverage for modern wireless communications. 5G communication should not only provide fast data rates but also offer a wide coverage area with outside to inside network coverage by using frequency bands below 10 GHz [5]. We can find some 5G antennas design and different feeding techniques with flexible materials papers [6-20] have been reviewed.

Arpan et al. [6], designed a flexible CPW-fed transparent antenna with a gain of over 3 dB and efficiency of over 80% for WLAN and sub-6 GHz 5G applications with an operating frequency range of 3.89-5.9 GHz, but the antenna size is large. Shivangi et al. [7], introduce a small microstrip patch antenna with a resonant frequency of 10.15 GHz for future 5G applications, where gain and bandwidth are quite poor because of omnidirectional characteristics. A compact antenna design for 5G wireless communications based on split ring resonators presented by Run long et al. [8], which operates at 3.5GHz with a relative bandwidth of 2.28% and a gain

of 7.43dB, but it is quite bulky. Elmobarak et al. [9], designed a transparent and flexible polymer-fabric tissue ultra-wideband antenna for future UWB wireless networks. This antenna has a good radiation pattern, but gain is poor because it resonates over several frequency bands. Rahim et al. [10], designed and fabricated a flexible wideband antenna for 5G applications that operate from 7-13 GHz and has an essentially omnidirectional radiation pattern with an average gain of 5 dBi, but the size of the antenna is larger. In work [11], a dual-band microstrip patch antenna array with excellent gain and return loss for 5G mobile communications. However, it's not cover the 5G lower band. In research [12], authors presented a small dual band antenna for sub-6 GHz 5G wireless applications with frequency bands of 3.29-3.63 GHz and 4.3-5.2 GHz with a peak gain of approximately 7.17 dBi where total bandwidth is lower according to its size. Huang et al. [13], proposed a split-ring double band base station antenna for sub-6 GHz communication which covers 2515 to 2675 MHz, 3400 to 3600 MHz, and 4800 to 5000 MHz, with an average gain of 8.2 dBi but return loss is lower. In the study [14], using a pair of ring dipoles and Y-shaped feeding lines, a wideband double split antenna for LTE/5G base applications has been proposed, which resonates at 3.3 GHz with 8.3dB stable gain. When one of the ring dipoles is excited, the parasitic element is considered to effectively extend the bandwidth, but the size is larger. Hua et al. [15], designed a small double band polarized base station. The double band performance is attained by including a small oval-shaped ring within the main oval-shaped ring while sustaining the size of the radiating patch constant. It operates at frequencies ranging from 3.3-3.8 GHz and 4.8-5.0 GHz. However, this antenna either covers the lower frequency band or, the higher frequency band. For wideband applications, a Fractal antenna in the Row shape of a was suggested [16]. The proposed antenna is constructed using 90° rotations in each iteration of a -shape around the base shape. For UWB applications, a planar antenna had been suggested [17]. The antenna consists of a square patch, a ground plane that is only partially covered, and a ground plane slot. A brand-new, small planar monopole UWB antenna with dual band-notched properties was introduced [18]. Four circled concave profiles are used in a U-shaped radiation patch corner with various modifications to the antenna ground plane to create a UWB. For fifth-generation (5G) and long-term evolution (LTE) communication applications, a low-profile multi-slotted patch antenna had been suggested [19]. A stepped patch and a ground plane made up the antenna under study. For sub-6GHz 5G communication applications, a circular patch planar ultra-wideband antenna was published [20]. There is no need for a lumped element or large system ground plane because the anticipated antenna is made up of a circular patch and a ground plane. In [21-26] author proposed some methods for slot antennas designed. They are cross-shaped slot coupler antenna, lopsided open slots in a circular patch antenna, C-shaped linked feed antenna with an L-shaped monopole slot having rectangular divergence, octave shaped slot antenna with U-shaped strips for ultra-

wideband applications, a square slot monopole radiator with L-shaped strip, a triple band slot antennas with a transformer, a fictional resonance wideband slot antenna, a slot antenna with a hexagonal design and two split rings, as well as a U-shaped slot, dual mode operation with inverted F-antennas, antenna with F-shaped slots and a deformed ground.

This research presented a novel dual-band monopole patch antenna for a 5G wireless application. The novelties of our proposed antenna are larger bandwidth with an excellent S_{11} characteristic and excellent impedance matching, better gain, and efficiency. The previous research was not concerned about antenna size. However, our proposed antenna is quite small and hence perfectly suited for 5G wireless communication. The proposed antenna has a dimension of $27.88 \times 23.67 \times 1.58 \text{ mm}^3$. The fabricated antenna covers two frequency ranges, which are 3.20-4.60 GHz and 5.10-9.90 GHz, respectively. In the simulation, the two prominent resonance frequencies are obtained at 3.75 and 7.20 GHz. However, the equivalent resonances in measurement are at 3.70 GHz and 7.1 GHz, respectively. The proposed antenna has a 4.18 dBi maximum gain and a 93% efficiency. The paper is arranged into different sections for the convenience of presentation. The introduction is given in section I. The design procedure and structure are explained in section II. Result analysis and discussion is placed in section III, and finally, the paper concludes in section IV.

2. Antenna design procedure and structure

This part of the antenna technique is divided into two sections. The first step is to configure the antenna's radiating patch, which normally requires measuring the patch's length and width in this part. For the design of this antenna radiating patch, the substrate's dielectric constant, height, and antenna resonance frequency are required. The essence of the feeding technique is the second. Basically, two feeding approaches are employed to construct this antenna: one is inset fed, and the other is the transformer feeding quarter-wave technique; therefore, the feeding technique of the quarter-wave transformer has been chosen as the feeding technique. For a seamless antenna to work properly, it must have a lower than -10 dB return loss in the desired frequency ranges. It may be done by changing the structure of the antenna patch and the ground. The selection of material plays a crucial part for the antenna to work at sub-6 GHz. In the proposed design, commercially available material copper has been used for making the patch and the ground plate. Moreover, the size of the proposed antenna's radiator plays an important role in increasing bandwidth.

The following formula provides the width (W) and length (L) of the monopole antenna's radiator based on the effective dielectric permittivity and resonant frequency[27]

$$\lambda = \frac{c}{fr} \quad (1)$$

$$W = \frac{\lambda}{100} \quad (2)$$

$$L = \frac{\lambda}{4} \quad (3)$$

$$\epsilon_{reff} = \frac{\epsilon_r + 1}{2} + \frac{\epsilon_r - 1}{2} \left[1 + 12 \frac{h}{W} \right]^{-2} \quad (4)$$

where c = Speed of light in free space, f_r = Resonant frequency, λ = Wavelength of corresponding resonance frequencies, ϵ_r = Relative permittivity of the substrate, and h = Height of the substrate.

For decades, Defected Ground Structure has been used to expand the bandwidth of microstrip patch antennas. The Defected Ground Structure is used to achieve a wider bandwidth or multiband as well as to reduce cross-polarized radiation. Generally, one or more deficiencies are generated by removing a specific part of dielectric materials from the ground, producing a steady wave effect under the band gap frequency and a rapid wave effect above the band gap frequency. Furthermore, for wider band or multiband applications, the antenna should have a wide working bandwidth, improved efficiency, the requisite antenna's radiation pattern, and a

higher gain. Hence, a unique dual band Y-shaped Defected Ground Structure-based low profile microstrip patch antenna has been proposed, and detailed features are described in this work.

A proposed dual-band monopole patch antenna for a 5G wireless application is shown in Fig. 1. The length and width of the microstrip antenna were determined using quarter web length, that is, $\lambda/4$ and $\lambda/100$, correspondingly, according to the microstrip antenna configuration. Table 1 shows the detailed dimensions of each section of the antenna structure, where L_s and W_s are the length and width of the antenna dielectric substrate. L and W are the length and width of the copper patch and ground plate, h is the thickness of the substrate, and the copper sheet on the back has the same length and width as the substrate. It may be done by modifying the shape of the antenna patch and the ground.

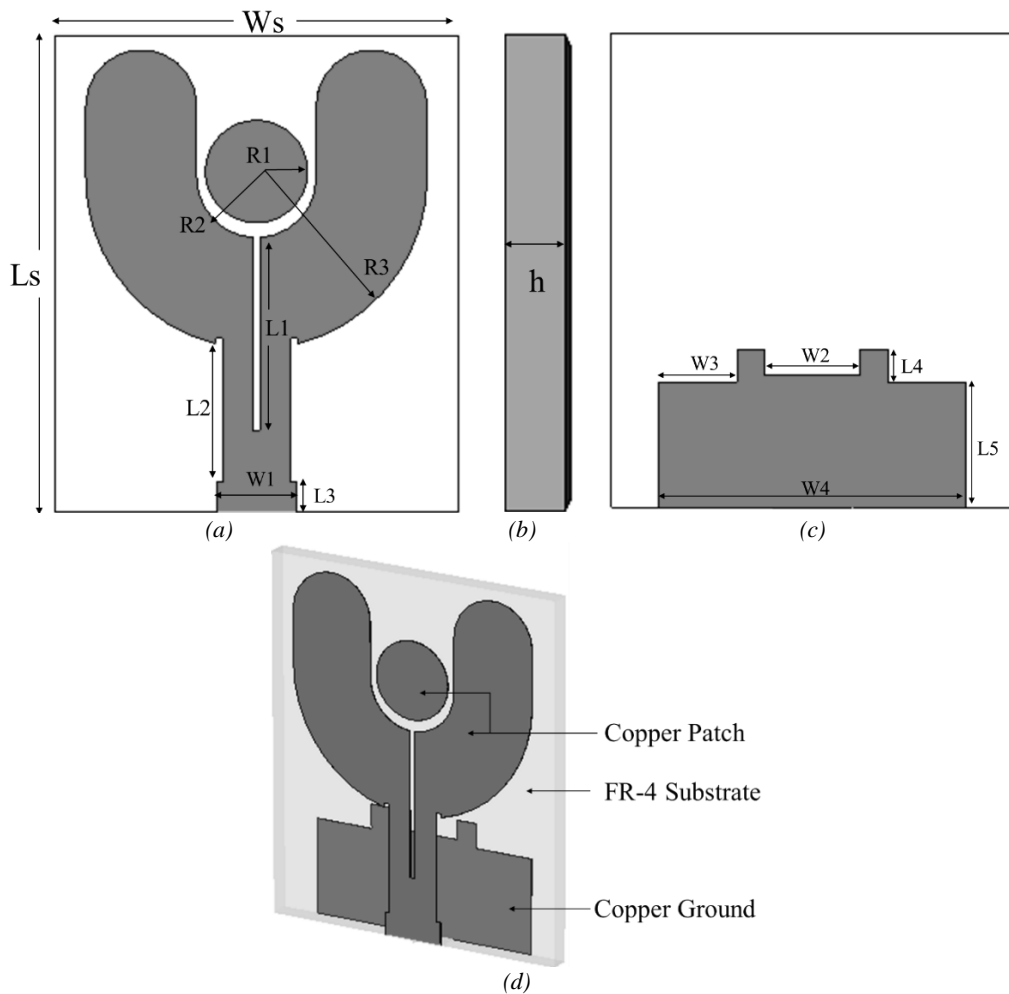


Fig.1 (a) Front view (b). Right view (c). Bottom view (d) Perspective view of the proposed antenna

Table 1. The parameters of the antenna are given below in "mm"

Parameter	Value	Parameter	Value	Parameter	Value	Parameter	Value
L_s	27.88	R_2	3.5	W_2	5.64	L_2	7.79
W_s	23.67	R_3	10	W_3	4.61	L_3	1.77
h	1.58	R_4	3.5	W_4	18.06	L_4	1.90
R_1	3	W_1	4.7	L_1	11.30	L_5	7.37

The antenna patch contains a Y-shaped plate at the top of the substrate. It also has a circular parasitic element in the middle of the Y-shaped plate, and the ground is a rectangular shape copper plate with two extra parts on the upper side of the ground. Copper has been used to make the patch and the ground. The copper plate has a thickness of 0.035mm and electric conductivity $\sigma=5.8e+07$ [S/m]. The height of the substrate is 1.58 mm, and it is made of Rogers RT5880 (lossy) material with Epsilon=2.2 Mu=1 Electric tend=0.0009 (Const. fit) Thermal conduct=0.2 [W/K/m] to provide a lossy environment.

Fig. 2 illustrates the simulated reflection coefficient and input impedance of the proposed antenna's three development steps. In the first step, we constructed a monopole patch antenna with a circle-shaped patch. The ground was designed with a rectangular-shaped copper plate and added two extra parts on top of the ground, but the reflection coefficient is unsatisfactory at this stage. Therefore, we improved our design to a satisfactory level. The second step involved reducing the return loss and shifting the resonance frequency to the required ranges. In this step, we modified it in a circle patch, where we cut half

of the radiator circle. The Fig. 2(a) graph shows that the antenna resonates at 4.4 GHz, but it's not covered our desired frequency ranges. Therefore, we modified it again to shift the resonance frequency to our required ranges. Step three added a Y-shaped copper plate on top of the substrate. A circular parasitic element is also added in the middle of the Y-shaped plate. We also see from the Fig. 2(a) that the antenna resonates at our desired frequency ranges. Finally, we proposed this step for our research work. On the other hand Fig. 2(b) show the z parameter graph of the various step for designing the proposed antenna. The Z-parameters can provide important information about the antenna performance, such as the input impedance, the resonant frequency, the bandwidth, and the radiation pattern. The input impedance can be adjusted by varying the dimensions of the patch or the feeding mechanism to match the impedance of the feed line or the RF source. The resonant frequency can be shifted by changing the dimensions of the patch or the substrate material. From Fig. 2(b) it can be clearly stated that proposed design input impedance real value near 50 ohm in the -10dB operating band and imaginary value near to 0.

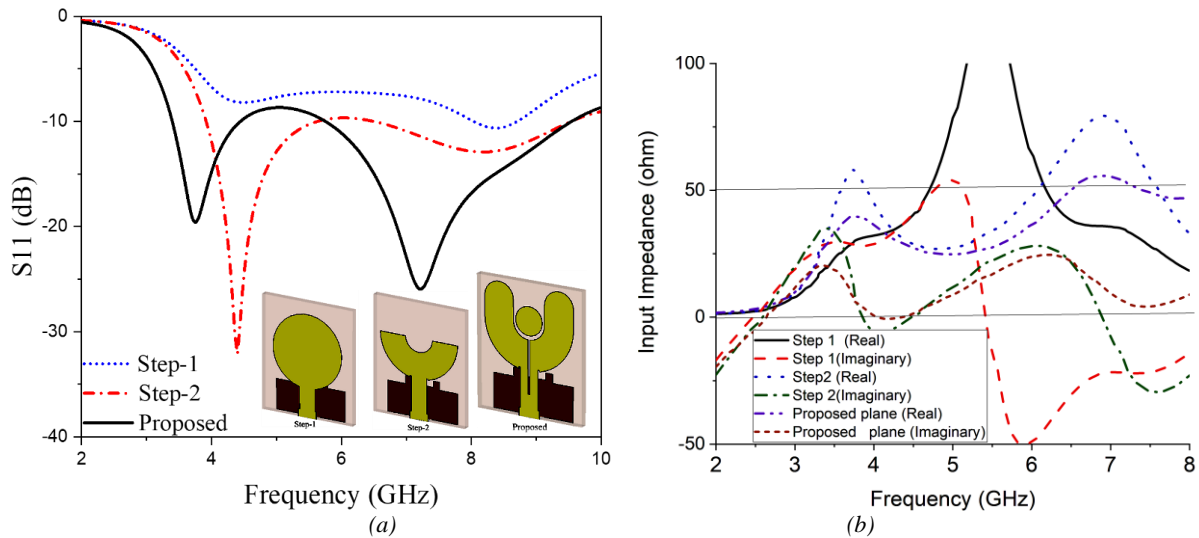


Fig. 2 (a) Reflection coefficient (b) Z Parameter (input impedance) of simulated antenna's evolution stages (color online)

Fig. 3 illustrates antenna design configurations for different ground heights. First of all, a full ground plane is chosen in Fig. 3 a, where the wide (Ws) and height (Ls) of the ground are 23.67 and 27.88 mm. Then we reduced the height of the ground from the full ground plan (27.88 mm) to the half ground plan (13.94 mm), which shows in Fig. 3 (b). On the other hand, Fig. 3 c, d shows the antenna design configuration with Defected Ground Structure and without Defected Ground Structure slot on the rectangular patch at its ideal height. The ground height L_5 value is considered as 9.27 mm, and the W_4 value is 18.06 mm for the design configuration shown in Fig. 3 c, where L_5 , W_2 , and W_3 values are nominated as 7.37 mm, 5.64 mm, and 4.61 mm for the layout shown in Fig. 3 (d), respectively.

It's clear from Fig. 4 that when the ground is the full plan, the reflection coefficient value is higher. Then when we reduce the height of the ground, the reflection coefficient is increased but unsatisfactory. At that time, when we reduced the width and height of the ground, as can be seen in the Fig. 4, the reflection coefficient curve crosses the -10 dB line at lower frequencies but it's not fulfilled our required band. So, the antenna's ground structure is finally improved to a partial ground plane constructed on DGS.

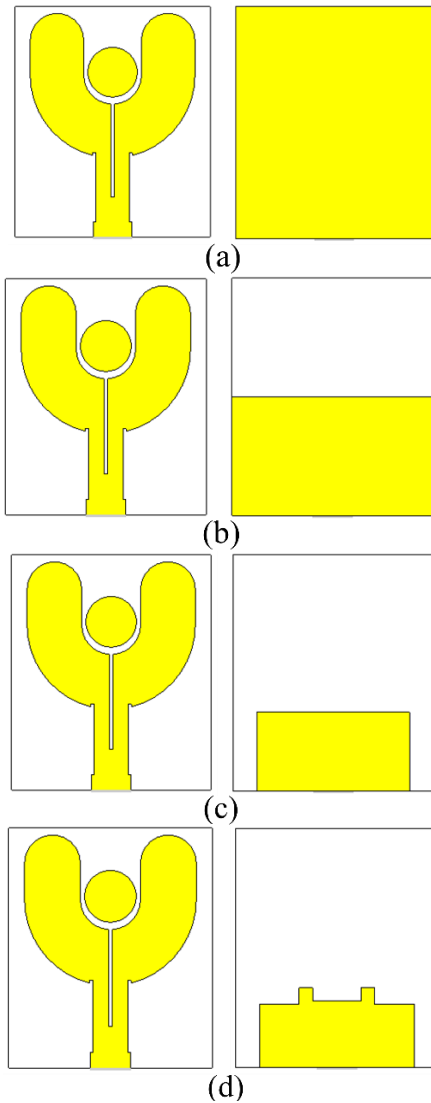


Fig. 3. Antenna design configuration by changing ground height (a) full ground (b) half ground (c) without defective ground structure slot (d) with defective ground structure slot (color online)

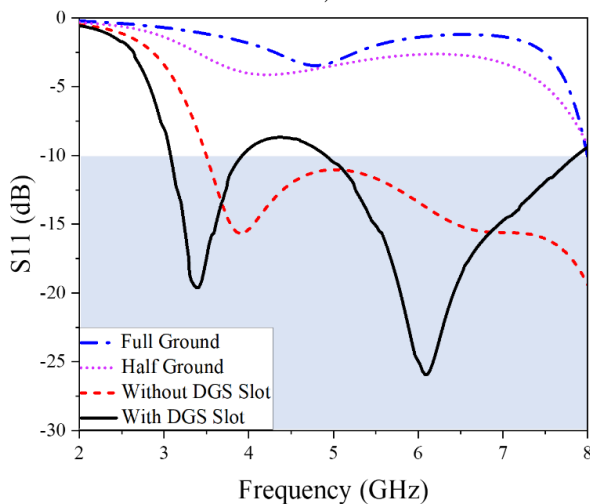


Fig. 4. Simulated reflection coefficient regarding ground height variation (color online)

3. Experimental results and discussion

Fundamental analysis of the proposed antenna design is performed using the CST studio suite. An antenna is completed in three stages: first, it's developed with simulation software, then it is fabricated, and finally, the antenna characteristics are measured. Using the scientific data plotting program Origin Pro, the simulation and measurement data are done for all plots. The simulated antenna is fabricated in our laboratory using a PCB milling machine known as the LPKF Proto Mat E33 after the simulation is completed. Fig. 3 depicts a prototype of the proposed antenna that has been fabricated and tested to ensure that the design is valid.

After prototyping, a PNA series vector network analyzer which a model number is N5227A has been used to evaluate the S_{11} parameters of the fabricated antenna shown in figure 4 a, where the gain and radiation patterns have been measured by using a Satimo Starlab system established in UKM lab, Malaysia shown in Fig. 4 b. To examine the effectiveness of an antenna, the reflection coefficient or S_{11} is the most basic parameter. The reflection coefficient provides data regarding the reflected energy of an antenna. The reflection coefficient vs. frequency graph makes it easy to determine the working frequency and antenna bandwidth. The stronger the antenna's resonance, the lower the parameter value of S_{11} . The simulated and measured reflection coefficient of the proposed antenna is shown in Fig. 5. It is clear from the figure that our proposed antenna engenders dual resonate modes, which resonate frequency range from 3.40-4.44 GHz and 5.80-9.56 GHz, respectively, when it's simulated. On the other hand, the measured resonate frequency ranges from 3.20-4.60 GHz and 5.10-9.90 GHz, sequentially. The dual resonate modes cover two Malaysian frequency bands, which are 3.5 GHz and 5.9-7.1 GHz, correspondingly with an excellent reflection coefficient of -23.30 dB and -26.60 dB, approximately when we verified this design.

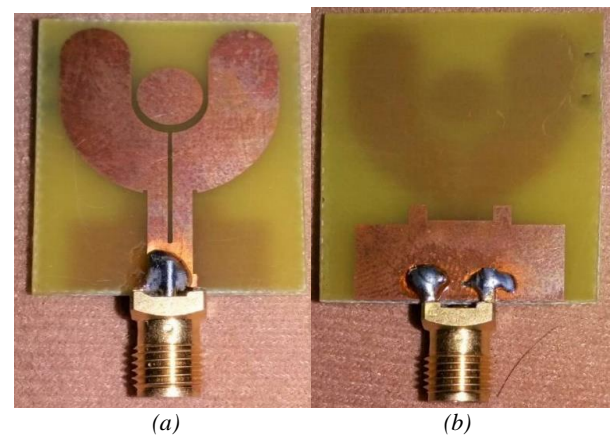


Fig. 5. Prototype of the proposed antenna (a) front view (b) back view (color online)

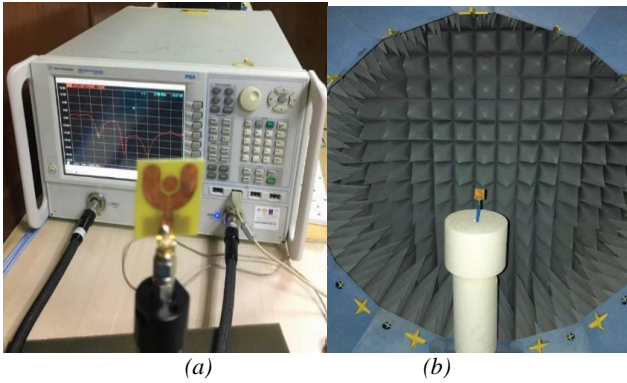


Fig. 4 (a) PNA network analyzer (b) Satimo StarLab (color online)

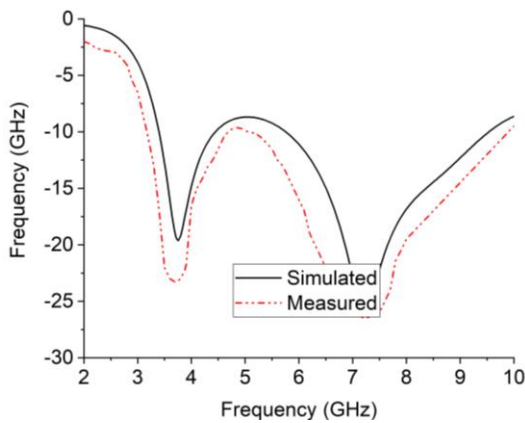


Fig. 5. Reflection coefficient of simulated and measured antenna (color online)

5G communication requires high directivity and gain to overcome attenuation and improve transmission range—the type of substrate material quality, substrate layer, and antenna size all effects antenna gain. The antenna's realized gain and efficiency are analyzed using Satimo StarLab. The simulated and measured gain and efficiency of the antenna shows in Fig. 6 a and Fig. 6 b, respectively. The results show that there is very little difference between the simulated and measured gain and efficiency. The measured results show that the maximum gain of the proposed antenna is 4.78 dBi which is in agreement with the simulated maximum gain of around 5.06 dB. For 5G wireless communication, efficiency should be more than 70%. The maximum efficiency which has been measured is 92 %. However, the simulated maximum efficiency is 94%. The result also reveals that the simulated and measured results are extremely well matched to each other. The designed and fabricated antenna's gain and efficiency can satisfy the specifications of a practical 5G wireless application.

Fig. 8 depicts the surface current distribution for the proposed antenna for two major resonance frequencies of 3.75 and 7.2 GHz, respectively. The surface current distributions were observed using the CST studio suite 2019. The current intensity is enhanced in all cases because of the defected ground structure slot on the

ground plane and the borders of the slope on the antenna's radiator. This change in current intensity has an impact on all of the antenna's characteristics. The most significant surface current conductive area of the antenna may be seen around the feed point and also the entire radiator of the antenna. For the proposed antenna, the slot at defective ground performed the most important role in obtaining dual band frequencies. The current distributions of the frequencies are different from each other. For example, surface currents appeared to concentrate on the upper section of the feed line and the wider radiator at the top border of the patch for the lower frequency band. On the other hand, the surface current density at the higher resonance frequency (7.2 GHz) is significantly larger than the current density observed at, the lower resonance frequency (3.75 GHz).

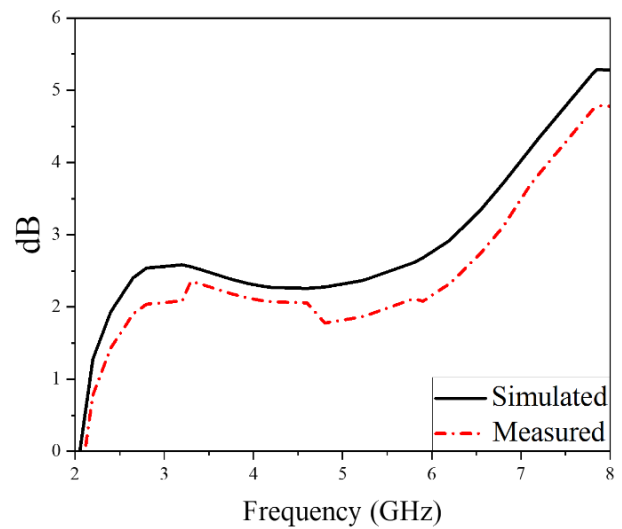


Fig. 6. Gain of the proposed antenna (color online)

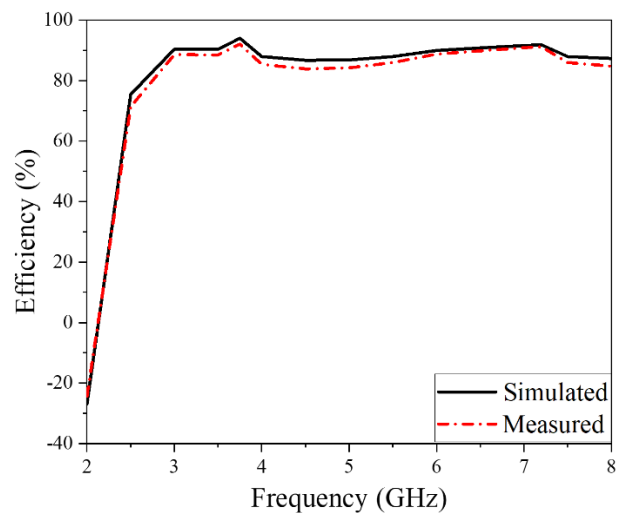


Fig. 7. Efficiency of the proposed antenna (color online)

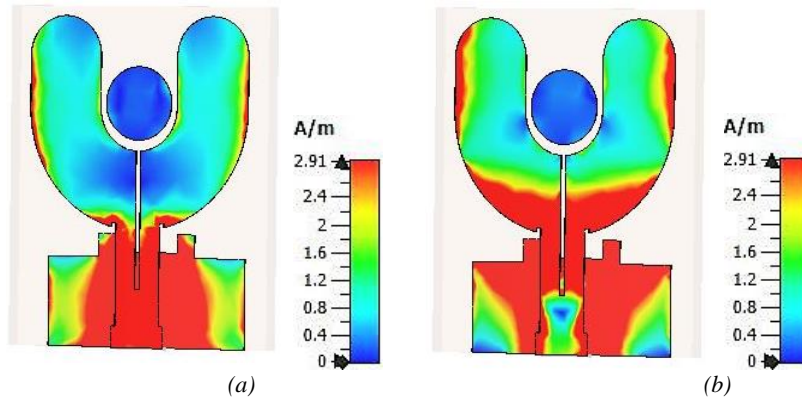


Fig. 8. Surface current distribution of the proposed antenna at (a) 3.75 GHz and (b) 7.20 GHz (color online)

Fig. 9 shows the simulated and measured 2D co-polarization and cross-polarization radiation patterns at two separate frequencies of 3.75 GHz and 7.20 GHz, respectively. For cartesian axis alignments, theta and phi are spherical coordinates, such as when phi is equal to constant 0° , then theta is equal to 0° to 360° degrees, known as the E-plane radiation pattern. In opposition, when phi is equal to a constant 90° , then theta is equal to 0° to 360° , known as the H-plane radiation pattern. The proposed design has an omnidirectional stable radiation pattern in co-polarization for E-plane radiation pattern of the frequency of 3.75 GHz and 7.2 GHz, respectively. The main lobe magnitude is 17.1 and 17.8 dB. The main lobe

direction is 180 and 0 degrees. In cross-polarization, the simulated angular width is 84.9 and 60.7 degrees, the sidelobe level is -3.4 and -1.1 dB, the main lobe magnitude is 17.1 and 19.5 dB, and the main lobe direction is 177 and 155 degrees, respectively. On the other hand, In co-polarization for H-plane radiation pattern of the frequency of 3.75 GHz and 7.2 GHz, correspondingly. The main lobe magnitude is -34.4 and -33.7 dB. The main lobe direction is 180 and 0 degrees. In cross-polarization, the simulated angular width is 84.9 and 60.7 degrees, the main lobe magnitude is -34.4 and -32.1 dB, and the main lobe direction is 177 and 155 degrees, correspondingly.

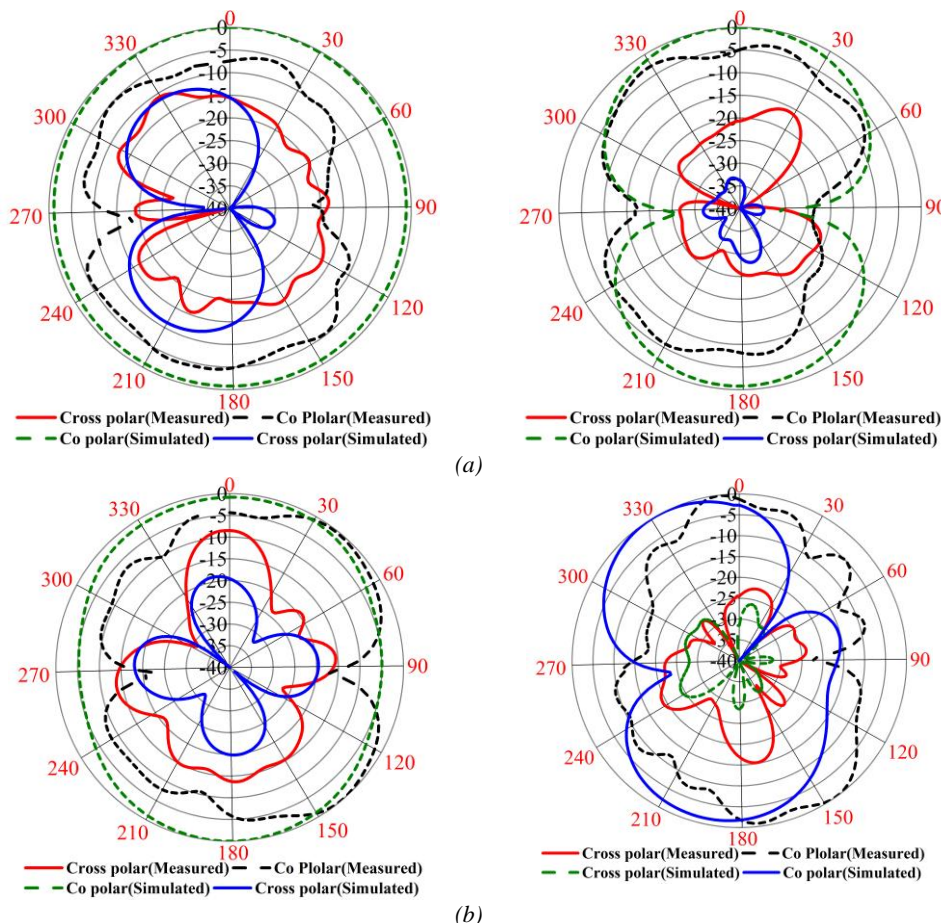


Fig. 9. E-Plane (left) and H-Plane (right) radiation patterns (a) 3.75 GHz (b) 7.2 GHz (color online)

The 3D Radiation pattern of the proposed antenna at two separate frequencies of 3.75 GHz and 7.20 GHz, respectively, are shown in Fig. 10. It is clear from the figure that the proposed antenna has a nearly omnidirectional radiation pattern. The azimuthal direction is where most of the radiation is focused. The figure shows

that the proposed antenna is directional with a gain of 2.44 dBi and 4.70 dBi, respectively, where the directivity is 2.62 dBi and 4.97 dBi, correspondingly. For 3.75 GHz, the total efficiency is -0.26 dB. On the other hand, the total efficiency is -0.32 for the frequency of 7.20 GHz.

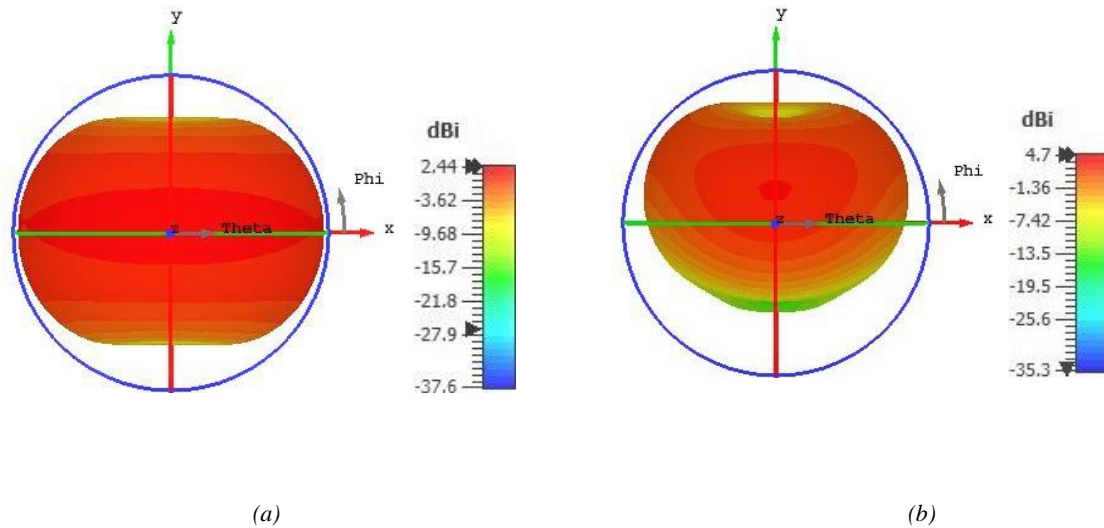


Fig. 10. 3D Radiation pattern of the proposed antenna at (a) 3.75 GHz and (b) 7.20 GHz

Table 2 makes the comparison clearer between the simulated and measured antennas. We compared the reflection coefficient, bandwidth, gain, directivity, and efficiency of the simulated antenna and measured the antenna in this table. The measured results are in good comparison with the simulated ones. The simulated bandwidths are 3.40-4.44 GHz and 5.80-9.56 GHz, respectively, with the reflection coefficient of -20 dB and -25 dB, correspondingly. On the other hand, the measured bandwidths are 3.20 to 4.60 GHz and 5.10 to 9.90 GHz, respectively, with the reflection coefficient of -23.30 dB and -26.60 dB, approximately the simulated gain is 4.75 dB, where the measured gain is 4.18 dB. The measurement shows that the antenna has 92% efficiency while the simulated efficiency is 94 %.

Table 3 shows the performance comparison with previously published research and our proposed research, where the size of the antenna, peak gain, efficiency, and operating bands are compared. It is clear from Table 3 that the presented antenna has higher performance in terms of small size compared to the reference antennas. In also comparison to earlier studies, the proposed antenna has a satisfactory gain and higher efficiency. It's also seen that most of the previous antennae attained a single band, but our proposed antenna achieved a dual band which covered two Malaysian frequency spectrums. However, the proposed design has a low profile, and its covered microwave frequency spectrum includes X-band, C-band, S-band, and SHF-band, making it a better solution for WLAN/WiMAX and 5G wireless applications.

Table 2. Comparison between the simulated antenna and fabricated antenna

Antenna	Frequency range (GHz)	Resonate point (GHz) / S_{11} (dB)	Total bandwidth (GHz)	Peak Gain (dB)	Directivity (dBi)	Maximum Efficiency (%)
Simulated antenna	3.40-4.44	3.75 (-20.00)	4.80	5.06	5.06	94
	5.80-9.56	7.20 (-25.00)				
Fabricated antenna	3.20-4.60	3.70 (-23.30)	6.20	4.78	4.54	92
	5.10-9.90	7.20 (-26.60)				

Table 3 Comparison between previous work and our proposed work

Reference	Year	Size (X×Y) mm ²	Electrical Size at Lowest Resonance Frequency (λ)	Peak Gain (dB)	Maximum Efficiency (%)	Operating Band (GHz)
[6]	2020	58×78	0.48 λ ×0.64 λ	3.00	80	3.89-5.97
[12]	2021	31×36	0.30 λ ×0.17 λ	7.17	80	3.29–3.63 4.39–5.2
[28]	2019	19.75×50	1.08 λ ×0.41 λ	2.90	90	0.5–6
[29]	2018	63 × 51.2	0.84 λ ×0.68 λ	5.3	64	2.5–5.5
[30]	2020	40×15	0.72 λ ×0.42 λ	4.70	88	0.7-0.96 1.6–5.5
[31]	2020	150 × 80	1.67 λ ×0.891 λ	6.00	90	3.34–5.0
[16]	2013	60×61	0.179 λ ×0.176 λ	2.5	n/a	0.88-2.72
This Work	2022	27.88×23.67	0.29λ×0.25λ	4.18	92	3.20-4.60 5.10-9.90

4. Conclusion

In this research, a compact Y-shape dual band antenna for 5G wireless application. The microstrip monopole antenna, which has a very small dimension of 27.88×23.67×1.58 mm³, was designed and prototyped. The radiator patch and ground of the antenna are fabricated on an FR-4 substrate. The antenna's performance has been simulated and measured in terms of S₁₁ parameters, peak gain, efficiency, and radiation characteristics. The proposed antenna achieves dual bandwidth with sufficient reflection coefficient, higher gain, and efficiency and exhibits steady omnidirectional radiation patterns, according to experimental verification. The simulated results show that the antenna performs well in the frequency ranges 3.20–4.60 GHz and 5.10-9.90 GHz, respectively. The peak gain of the antenna is 4.16 dBi with an excellent reflection coefficient of -26.5 dB. The antenna has 92 % efficiency for the whole frequency band and provides 620 MHz of total bandwidth. Finally, the proposed antenna seems to be an attractive option for 5G wireless applications.

Acknowledgments

This work is supported by the Ministry of Science and Technology (MOST), Bangladesh research grant code: **SRG-222428**.

References

- [1] J. Thompson, X. Ge, H.-C. Wu, R. Irmer, H. Jiang, G. Fettweis, S. Alamouti, IEEE Communications Magazine **52**, 62 (2014).
- [2] N.-W. Liu, L. Zhu, W.-W. Choi, X. Zhang, IEEE Transactions on Antennas and Propagation **65**, 1055 (2017).
- [3] Z. Yu, Z. Lin, X. Ran, Y. Li, B. Liang, X. Wang, International Journal of Antennas and Propagation **2021**, 1 (2021).
- [4] X. Zhu, J. Zhang, T. Cui, Z. Zheng, International Journal of Antennas and Propagation **2019**, 4345819 (2019).
- [5] T. Wang, G. Li, J. Ding, Q. Miao, J. Li, Y. Wang, IEEE Communications Magazine **53**, 58 (2015).
- [6] A. Desai, T. Upadhyaya, J. Patel, R. Patel, M. Palandoken, Microwave and Optical Technology Letters **62**, 2090 (2020).
- [7] S. Verma, L. Mahajan, R. Kumar, H. S. Saini, N. Kumar, 2016 5th International Conference on Reliability, Infocom Technologies and Optimization (trends and future directions) (ICRITO), 2016, p. 460.
- [8] R. Li, Q. Zhang, Y. Kuang, X. Chen, Z. Xiao, J. Zhang, 2019 Cross Strait Quad-Regional Radio Science and Wireless Technology Conference (CSQRWC), 2019, p. 1.
- [9] H. A. E. Elobaid, S. K. A. Rahim, M. Himdi, X. Castel, M. A. Kasgari, IEEE Antennas and Wireless Propagation Letters **16**, 1333 (2016).
- [10] M. Tighezza, S. Rahim, M. Islam, Microwave and Optical Technology Letters **60**, 38 (2018).
- [11] U. Rafique, H. Khalil, 2017 Progress in Electromagnetics Research Symposium-Fall (PIERS-FALL), 2017, pp. 55.
- [12] I. Ishteyaq, I. S. Masoodi, K. Muzaffar, International Journal of Microwave and Wireless Technologies **13**, 469 (2021).
- [13] B. Huang, J. Cao, W. Lin, J. Zhang, G. Zhang, F. Wu, International Journal of Antennas and Propagation **2021**, 4657540 (2021).
- [14] B. Wang, C. Zhu, C. Liao, W. Luo, B. Yin, P. Wang, Electromagnetics **40**, 13 (2020).
- [15] Q. Hua, Y. Huang, A. Alieidin, C. Song, T. Jia, X. Zhu, IEEE Access **8**, 63710 (2020).
- [16] M. A. Dorostkar, R. Azim, M. Islam, Procedia Technology **11**, 1285 (2013).
- [17] R. Azim, A. T. Mobashsher, M. T. Islam, N. Misran, 2010 International Conference on Microwave and Millimeter Wave Technology, 2010, p. 1987.
- [18] A. A. H. Siddique, R. Azim, M. T. Islam,

- International Journal of Microwave and Wireless Technology **11**, 711 (2019).
- [19] R. Azim, A. M. H. Meaze, A. Affandi, M. M. Alam, R. Aktar, M. S. Mia, International Journal of Microwave and Wireless Technology **13**, 486 (2021).
- [20] R. Azim, R. Aktar, A. Siddique, L. Paul, M. Islam, J. Optoelectron. Adv. M. **23**(3-4), 127 (2021).
- [21] Z. Zhou, Z. Wei, Z. Tang, Y. Yin, IEEE Antennas and Wireless Propagation Letters **18**, 722 (2019).
- [22] M.-Y. Li, Y.-L. Ban, Z.-Q. Xu, G. Wu, K. Kang, Z.-F. Yu, IEEE Transactions on Antennas and Propagation **64**, 3820 (2016).
- [23] X. Dong, Z. Liao, J. Xu, Q. Cai, G. Liu, Progress in Electromagnetics Research Letters **46**, 101 (2014).
- [24] W. Hu, X. Liu, S. Gao, L.-H. Wen, L. Qian, T. Feng, R. Xu, P. Pei, Y. Liu, IEEE Access **7**, 178476 (2019).
- [25] R. Azim, M. T. Islam, H. Arshad, M. M. Alam, N. Sobahi, A. I. Khan, IEEE Access **9**, 5343 (2020).
- [26] M. T. Tan, J. Q. Li, Z. Y. Jiang, International Journal of RF and Microwave Computer-Aided Engineering **29**, e21935 (2019).
- [27] C. A. Balanis, Antenna theory: analysis and design, John Wiley & Sons, 2016.
- [28] N. Sekeljic, Z. Yao, H.-H. Hsu, 2019 IEEE International Symposium on Antennas and Propagation and USNC-URSI Radio Science Meeting, 2019, p. 147.
- [29] W. An, Y. Li, H. Fu, J. Ma, W. Chen, B. Feng, IEEE Antennas and Wireless Propagation Letters **17**, 621 (2018).
- [30] Z. An, M. He, The Applied Computational Electromagnetics Society Journal (ACES), 10 (2020).
- [31] M. Khalifa, L. Khashan, H. Badawy, F. Ibrahim, Journal of Physics: Conference Series, 012049 (2020).

*Corresponding authors: naimur.cse4th@pstu.ac.bd;
tariqul@ukm.edu.my;
sobuz@pstu.ac.bd